Neurobiology of Disease 134 (2020) 104666

Contents lists available at ScienceDirect

Neurobiology of Disease

journal homepage: www.elsevier.com/locate/ynbdi

Dopamine regulates spine density in striatal projection neurons in a concentration-dependent manner

Samuel Alberquilla[a], Aldo Gonzalez-Granillo[a,c,d], Eduardo Daniel Martín[a,1], Rosario Moratalla[a,b,*,1]

[a] Instituto Cajal, Consejo Superior de Investigaciones Científicas (CSIC), 28002 Madrid, Spain
[b] Centro de Investigación Biomédica en Red sobre Enfermedades Neurodegenerativas, Instituto de Salud Carlos III, 28031 Madrid, Spain
[c] Laboratorio de neuropsiquiatría, Instituto de Fisiología, Benemérita Universidad Autónoma de Puebla, México
[d] Laboratorio de Fisiología de la Conducta, Escuela Nacional de Ciencias Biológicas, Instituto Politécnico Nacional, Mexico

ARTICLE INFO

Keywords:
Dopamine
Striatum
Spines
Spiny projection neuron
Voltammetry
Parkinson's disease
Synaptic plasticity

ABSTRACT

Dopaminergic afferents innervate spiny projection neurons (SPNs) in the striatum, maintaining basal ganglia activity. The loss of striatal innervation is the hallmark of Parkinson's disease (PD), which is characterized by dopaminergic denervation. A lack of dopamine in the dorsal striatum induces plasticity changes in SPNs. However, PD-associated denervation is progressive, and how plasticity is modified in partially innervated areas is poorly understood. The most studied models of PD are based on the use of neurotoxins that induce an almost complete striatal denervation. To investigate the impact of partial dopamine (DA) innervation in striatal plasticity, we use a genetic model of PD, Aphakia (Ak) mice, whose striatum presents an increasing dorso-ventral gradient of dopamine innervation. We studied SPNs in three different areas (dorsal, middle and ventral, with low, moderate and high innervation by tyrosine hydroxylase TH-positive axons, respectively) using fast scan cyclic voltammetry, microiontophoresis, immunohistochemistry and patch clamp techniques. Our data show an increasing dorso-ventral gradient of extracellular DA levels, overlapping with the gradient of TH innervation. Interestingly, spine loss in both direct (d-SPN) and indirect SPNs (i-SPN) decreases from dorsal to ventral in the parkinsonian striatum of Ak mice, following the decrease in DA levels. However, their dendritic trees and the number of nodes are only reduced in the poorly innervated dorsal areas and remain unaltered in moderate and highly innervated areas. The firing rate of direct SPNs does not change in either moderate or highly innervated areas, but increases in poorly innervated areas. In contrast, action potential frequency of indirect SPNs does not change along the dorso-ventral innervation gradient. Our findings indicate that spine density in d-SPNs and i-SPNs varies in a dopamine concentration-dependent manner, indicating that both d- and i-SPN are similarly innervated by DA.

1. Introduction

The striatum is essential for action selection, modulating the control and integration of movement and non-motor functions, such as cognitive processes and limbic functions. The striatum is the major input nucleus of the basal ganglia. It receives dopaminergic innervation from the substantia nigra pars compacta (SNc) and ventral tegmental area (VTA) and glutamatergic innervation from the cortex and thalamus. The striatum is mainly formed by spiny projection neurons (SPNs), which are categorized into two types. The neurons that express dopamine D1 receptors (D1R) form the direct pathway (d-SPN) and facilitate motor behavior. Those that express D2 receptors (D2R) form the indirect pathway (i-SPN) and inhibit movements (Albin et al., 1989; Kravitz et al., 2010). Both types of neurons are GABAergic and exhibit low firing rates and low excitability because of their high threshold for action potentials.

The loss of striatal innervation or the axospinous synapses that carry motor information from dopaminergic neurons is the hallmark of Parkinson's disease (PD). Loss causes major synaptic dysfunction, with marked dendritic tree atrophy and a severe decrease in spine density in both d- and i-SPNs in the striatum (Day et al., 2006; Solís et al., 2007; Villalba et al., 2009; Fieblinger et al., 2014; Nishijima et al., 2014; Suarez et al., 2014, 2016, 2018; Toy et al., 2014; Gagnon et al., 2017; Lieberman et al., 2018; Graves et al., 2019). However, it remains

* Corresponding author at: Instituto Cajal, Consejo Superior de Investigaciones Científicas (CSIC), 28002 Madrid, Spain.
E-mail address: moratalla@cajal.csic.es (R. Moratalla).
[1] Equal contribution.

https://doi.org/10.1016/j.nbd.2019.104666
Received 15 July 2019; Received in revised form 24 October 2019; Accepted 31 October 2019
Available online 01 November 2019
0969-9961/

unknown whether the moderate DA levels in partially denervated/innervated striatal areas are able to trigger these changes and modify the synaptic morphology and intrinsic properties of SPNs.

We hypothesized that nigrostriatal dopaminergic innervation is directly associated with changes in the morphology and physiology of SPNs according to the extracellular levels of DA. To test this, we took advantage of Pitx3$^{-/-}$ aphakia (Ak) mice that, due to the selective lack of SNc DA neurons in the midbrain, present an increasing dorso-ventral gradient of dopaminergic innervation (Smidt et al., 2004). Pitx3 is a transcription factor expressed by midbrain DA neurons and is important for their terminal differentiation and survival. In Ak mice, the few Pitx3-independent DA neurons able to survive provide a gradient of striatal DA innervation increasing from dorsal to ventral, a state that is associated with motor impairments and other related signs of Parkinson's disease (Solís et al., 2015; García-Montes et al., 2018). This mouse line has been established as a model of moderate PD (Solís et al., 2015). Notably, the synaptic alterations and plasticity changes in patients (McNeill et al., 1988; Zaja-Milatovic et al., 2005) and in completely denervated striatal areas in PD mouse models (Graves et al., 2019) are also reproduced in Ak mice (Solís et al., 2015; Suarez et al., 2018; Lieberman et al., 2018).

2. Methods

2.1. Animals

This study was carried out in 1- to 3-month-old male hemizygous BAC-transgenic mice (D1R-tomato and D2R-eGFP, C57BL/6) crossed with WT or with homozygous Pitx3$^{-/-}$ (C57BL/6) or Ak mice. Red tomato and green GFP fluorescence were used to identify d-SPNs and i-SPNs, respectively. Animals were group-housed and kept on a 12 h light/dark cycle with ad libitum access to food and water. All procedures were performed in accordance with the guidelines from European Union Council Directive (86/609/European Economic Community).

3. Brain slice preparation

Mice were anesthetized and transcardially perfused with artificial cerebrospinal fluid (aCSF) that contained: 124 mM NaCl, 2.69 mM KCl, 1.25 mM KH_2PO_4, 2 mM $MgSO_4$, 26 mM $NaHCO_3$, 10 mM D-glucose, and 2 mM $CaCl_2$ at pH 7.4. Coronal brain slices (400 µm thick) of neostriatum were prepared using conventional methods (Oliva et al., 2013), and incubated in a holding chamber at room temperature (21–24 °C) in aCSF and gassed with carbogen (95% O_2 and 5% CO_2).

3.1. Fast-scan cyclic voltammetry

Fast-scan cyclic voltammetry (FSCV) recordings were performed in three different areas of striatal slices following the dorso-ventral axes corresponding to the dorsal striatum (s1-s3), middle striatum (s4-s6) and the ventral striatum (s7-s9). FSCV at the carbon fiber electrode (CFE; 10 µm diameter; 50 µm exposed length) was used to detect changes in extracellular concentrations of DA following a puff of KCl (400 mM). FSCV was carried out using three electrode voltage-clamp amplifiers (VAMP-1, Registim LLC, Coral Gables, FL, USA) as previously described (Granado et al., 2011; Ares-Santos et al., 2012; Oliva et al., 2013). CFE was used as the working electrode, Ag/AgCl pellet as the reference electrode and a platinum wire as the auxiliary electrode. A voltage scan rate of 400 V/s was applied consecutively every 200 ms to the CFE. Changes in extracellular DA were determined by monitoring the current at the peak oxidation potential for DA. Background-subtracted cyclic voltammograms were created by subtracting the current before stimulation from the current in the presence of DA (Fig. 1C). Current was digitized at 10 kHz using a PowerLab 4/25 T (AD Instruments, Bella Vista, Australia) acquisition system. Data were acquired and analyzed with Scope software (AD Instruments). Electrodes were calibrated with DA standards of known concentration (0.5, 1, 2, 3 and 5 µM DA) in the recording chamber. The average of set of measurements was used as the calibration factor.

3.2. Electrophysiology

Whole-cell electrophysiological recordings were performed as previously described (Martin et al., 2012) in three different areas of striatal slices following the dorso-ventral axes corresponding to the dorsal striatum (s1-s3), middle striatum (s4-s6) and the ventral striatum (s7-s9). Patch pipettes were pulled from thick-walled borosilicate glass with a model P-97 micropipette puller (Sutter Instruments, Novato, CA). Pipettes (3–5 MΩ) were filled with the internal solution that contained: 100 mM K-Gluconate, 32.5 mM KCl, 10 mM HEPES, 5 mM EGTA, 1 mM $MgCl_2$, 4 mM ATP-Na_2 and 0.4 mM GTP-Na_2 (pH adjusted to 7.3 with KOH). Slices were transferred to an immersion recording chamber and continuously perfused with aCSF solution gassed with carbogen (95% O2 and 5% CO2). d-SPNs (red) and i-SPNs (green) were identified under fluorescence illumination. Electrophysiological recordings were obtained using a Multiclamp 700B amplifier and analyzed using a digital system (pClamp version 11.0, Molecular Devices). Excitability was obtained using 500 ms somatic current injection in current clamp mode.

3.3. Single-cell microinjection and immunohistochemistry

Animals were anesthetized with sodium pentobarbital (50 mg/kg, i.p.) and transcardially perfused with 4% paraformaldehyde (pH 7.4). Brains were post-fixed for 24 h in the same solution. Coronal sections were obtained on a vibratome (Leica, RRID: SCR_008960). The cutting sequence was 200 and 30 µm thick sections throughout the entire striatum, following the protocol previously described by Suarez et al. (2014; Supplementary Fig 1). 200 µm sections were used for Lucifer Yellow injections and morphological reconstruction of SPNs. d-SPNs (red fluorescence) and i-SPNs (green fluorescence) were impaled with a micropipette containing 8% Lucifer Yellow (Sigma-Aldrich), injected with 10–20 nA of hyperpolarizing current, and slices were processed for immunocytochemistry with the anti-Lucifer Yellow antibody (1:100,000; kindly provided by Dr. De Felipe, CSIC) as described previously (Suarez et al., 2014, 2016, 2018). Neurolucida v8 (MicroBrightField RRID: SCR_001775) was used to trace 3-dimensional dendritic arbors of SPNs and to mark spines. To determine in which striatal region each neuron was positioned, 30 µm sections were used for TH (1:1000; Millipore AB1542, RRID: AB_11213126). Immunofluorescence micrographs were obtained using confocal microscopy (Leica) at 63 × .

3.4. Quantitative assessment of dopaminergic fibers in the striatum

For the analysis of dopaminergic fibers in the striatum, we used an image analysis program (ImageJ) to convert color intensities into a gray scale. Striatal sections were taken with an optical microscope with a 4× lens. To choose the threshold that would be applied to all the groups, we use an average of WT slices in which the amount of TH fibers was maximum (around 100%) and was applied to Ak animals to determine the % TH fibers. We measured the area of staining in the striatum as the proportion of pixels in the striatum that show staining relative to the total pixels in the striatum (Ares-Santos et al., 2014).

3.5. Statistics

FSCV, % TH fibers, total dendritic length and distal spines were analyzed using one-way ANOVA followed by the Bonferroni post-hoc test. Electrophysiological and Sholl analyses were conducted using two-way ANOVA followed by the Bonferroni post-hoc test. Analysis was performed with GraphPad Prism 5 (La Jolla). Data are expressed as the mean ± standard error of the mean (SEM).

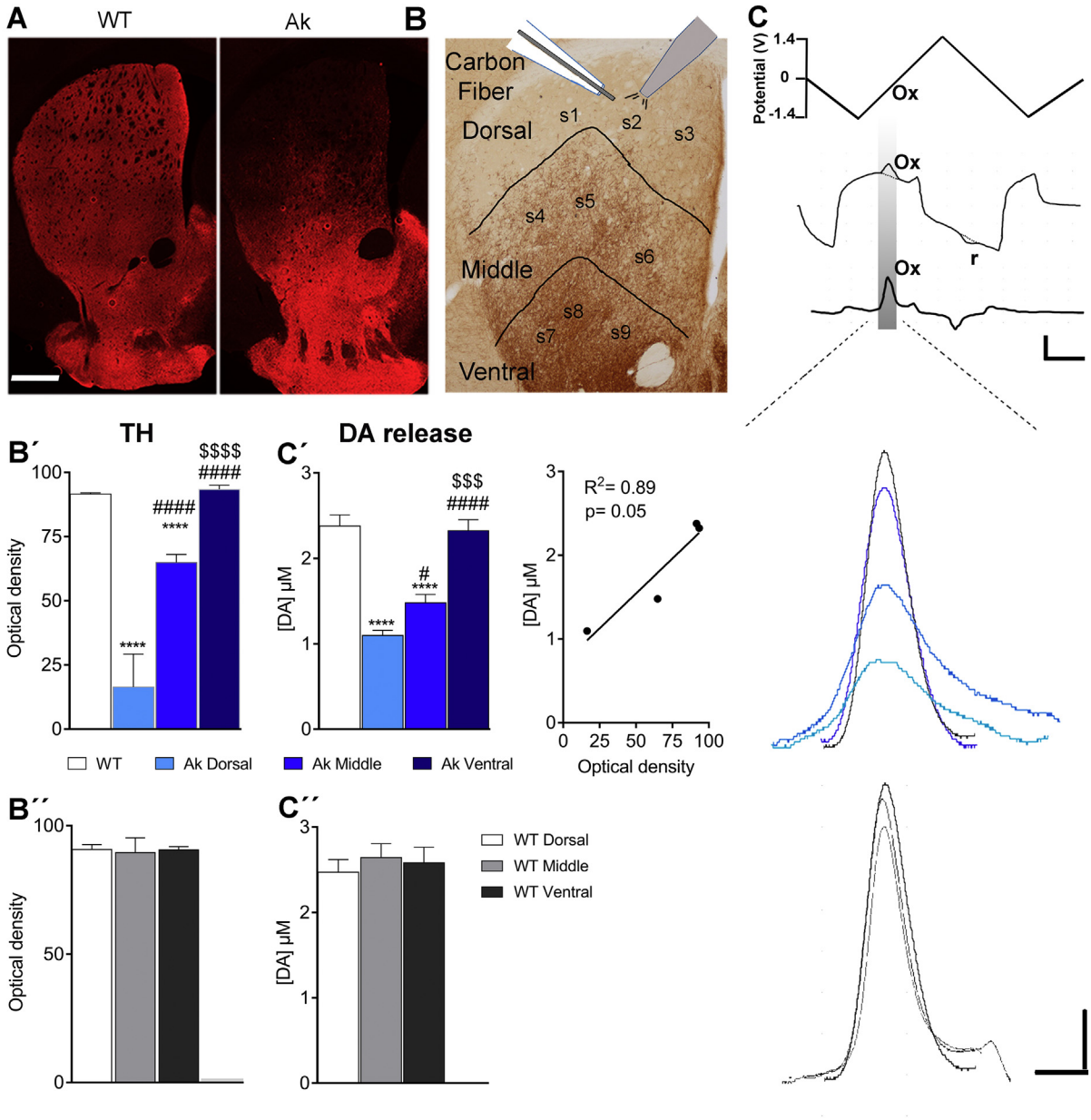

Fig. 1. Ak mice show an increasing striatal dorso-ventral gradient of extracellular DA levels correlating with TH innervation. Striatal coronal sections of WT and Aphakia mice stained with TH illustrating the striatal gradient of dopamine innervation in Ak mice (A) and the location of the carbon fiber and KCl pipette for recording sites in the dorsal, middle and ventral striatal areas, corresponding to low, moderate and high TH-innervation, respectively (B). (C) Top, the applied voltage to the carbon fiber consists of a triangular waveform with a voltage scan rate of 400 V/s. Middle, the current evoked by the input voltage at the carbon fiber. When DA is in the extracellular medium, there is an increase in the current due to its oxidation (o) and reduction (r). Bottom, background-subtracted voltammograms and representative peak of DA in the three different striatal areas of Ak and WT mice. (B′, B″) Histograms represent mean percentage of TH innervation measured as optical density in the three striatal areas in Ak mice, n = 15 slices, (B′) and WT mice, n = 9 slices, B". (C′, C″) Mean peak dopamine concentrations in the dorsal (n = 35 slices, s1-s3), middle (n = 38 slices, s4-s6) and ventral (n = 9 slices, s7-s9) areas of Ak and correlation analysis showing the relationship between TH innervation and DA overflow (C′). Mean peak of dopamine concentrations in WT mice (C″) (n = 34 slices).
Significant differences were established by one-way ANOVA followed by Bonferroni's test at $^{****}p < .0001$ vs. WT; $^{\#}p < .05$, $^{\#\#\#\#}p < .0001$ vs. Ak Dorsal; $^{\$\$\$}p < .001$, $^{\$\$\$\$}p < .0001$ vs. Ak Middle. Scale bar: 500 µm, A; 300 nA and 400 ms, C top; 0.5 µM DA and 500 ms, C bottom.

4. Results

4.1. Aphakia mice show a dorso-ventral gradient of extracellular DA levels correlating with TH innervation

Ak mice show a dorso-ventral gradient of dopamine innervation in the striatum (Smidt et al., 2004; Solís et al., 2015; Suarez et al., 2018) with ventral areas more innervated than dorsal areas, where only a few TH fibers remain (Fig. 1A, B). In order to test whether the extracellular DA levels matches the dorso-ventral gradient of dopaminergic innervation, we quantified TH fibers along the dorso-ventral striatal axis by optical density. This quantification allowed us to divide the striatum into three different areas: dorsal with just 16.41% ± 3.31 TH fibers; middle with 64.91% ± 3.12 and ventral with 93.41% ± 1.60 (Fig. 1B, B'). Such a TH gradient was not observed in the WT, in which the values ranged from 90.79% ± 1.86 for dorsal, 89.6% ± 5.67 for middle and 90.59% ± 1.24 for ventral striatum (Fig. 1B").

To know if the extracellular DA levels in Ak mice correlated with the dorsoventral gradient of dopaminergic innervation, we recorded from these three selected areas, at three different sites (s1, s2, s3, etc) per

area, using FSCV to measure dopamine overflow (Fig. 1B, C). This method allows us to detect electrochemically active neurotransmitters based on their oxidation and reduction properties (Armstrong-James and Millar, 1979). In parallel with the TH fiber innervation, we found that the dorsal striatum of Ak mice present low extracellular DA levels (1.2 μM ± 0.06), followed by the middle and ventral areas (1.61 μM ± 0.1 and 2.19 μM ± 0.16, respectively; Fig. 1C'), while extracellular DA levels in WT mice does not change along the dorso-ventral axis (dorsal 2.47 μM ± 0.15, middle 2.64 μM ± 0.16 and ventral 2.58 μM ± 0.18; Fig. 1C''). Additionally, correlation analysis shows the relationship between TH innervation and extracellular DA levels. Our results show that there is a gradient of extracellular DA levels along the dorso-ventral striatal axis in Ak mice, which follows the dorso-ventral gradient of TH fibers.

4.2. SPN morphology is modified along the dorso-ventral striatal axis of Aphakia mice according to DA concentration

The morphological plasticity of projection neurons in completely denervated dorsal striatal areas has been intensively studied using different mouse models of PD (Fieblinger et al., 2014; Suarez et al., 2014, 2016, 2018; Graves and Surmeier, 2019). Yet, although PD is progressive, the structural synaptic changes of SPNs in partially denervated striatal areas and how these changes occur has never been addressed. Here, in order to see how different DA levels affect synaptic plasticity, we studied whether spine density and dendritic morphology of SPNs follow the dorso-ventral gradient of extracellular DA levels and TH fiber innervation in the striatum of Ak mice (Fig. 2). We analyzed the morphology of SPNs with Lucifer yellow (LY) microiontophoresis in the three differently innervated striatal areas in 200 μm thick slices (Fig. 2A). To distinguish between the three areas in the 200 μm slices, we used adjacent slices (30 μm thick) stained with TH as depicted in Fig. 2B, C.

We found that dendritic arborization was not significantly modified in the middle (2749 μm ± 255.6 for d-SPNs, 2074 μm ± 181.3 for i-SPNs) or ventral striatum (2870 μm ± 341 for d-SPNs, 1944 μm ± 270.7 for i-SPNs). However, the dendritic arborization of both d-SPNs (1599 μm ± 157.5) and i-SPNs (962.7 μm ± 72.49) in the dorsal striatum of Ak mice was decreased compared to WT (measured as the mean of the three striatal regions; 2320 μm ± 104.4, 1789 μm ± 204.3; Fig. 3 A, B). In addition, only in the poorly innervated areas was there a reduction in the number of nodes in both d-SPN and i-SPN (d-SPN: 18.07 ± 1.26, WT; 13.32 ± 0.92, Ak dorsal; 18.42 ± 1.39, Ak middle and 20.42 ± 2.02, Ak ventral; i-SPN: 16.07 ± 2.04, WT; 9.68 ± 0.77, Ak dorsal; 17.33 ± 1.25, Ak middle and 16.42 ± 1.25, Ak ventral; Fig. 3C). However, we did not find significant differences in the number of primary dendrites in SPNs (Fig. 3D) along the dorso-ventral innervation gradient. Because there is no differential gradient of DA or TH across the striatum in WT mice we tested that DA does not regulates the total length SPN (d-SPN: 2428 μm ± 191.3, WT dorsal; 2220 μm ± 180, WT middle and 2325 μm ± 189.1, WT ventral; i-SPN: 1823 μm ± 253.9, WT dorsal; 1963 μm ± 311.7, WT middle and 1585 μm ± 472.9, WT ventral) nodes (d-SPN: 16.75 ± 1.84, WT dorsal; 18.6 ± 2.64, WT middle and 18.67 ± 1.97, WT ventral; i-SPN: 19.4 ± 4.65, WT dorsal; 15 ± 3.05, WT middle and 13.8 ± 5.64, WT ventral) or primary dendrites (d-SPN: 7.43 ± 0.87, WT dorsal; 7.75 ± 0.45, WT middle and 8 ± 0.52, WT ventral; i-SPN: 6.8 ± 0.49, WT dorsal; 7 ± 0.89, WT middle and 9.2 ± 1.24, WT ventral) in both SPNs in a concentration-dependent manner (Figure supplementary 1).

This suggests that even moderate DA levels are sufficient to maintain the dendritic tree and nodes in the striatal neurons.

Next, we measured the spine density in the proximal (< 45 μm) and distal parts of the dendrites (from 45 μm onwards). We did not find differences in the proximal spine density in both SPNs of WT mice along the dorso-ventral axis (dSPN: 2.68 ± 0.61, WT dorsal; 2.95 ± 0.56, WT middle and 2.34 ± 0.62, WT ventral; iSPN:: 2.23 ± 0.51, WT dorsal; 3.09 ± 0.53, WT middle and 2.95 ± 0.76, WT ventral); Figure supplementary 2. Curiously, we found a reduction in the proximal spine density in both d-SPNs and i-SPNs in Ak mice (d-SPN: 1.44 ± 0.19 for dorsal; 1.07 ± 0.17, middle and 1.34 ± 0.15 in the ventral striatum compared to 2.37 ± 0.30 in the WT mice; i-SPN: 1.43 ± 0.27 for dorsal; 1.28 ± 0.31, middle and 1.57 ± 0.19 ventral compared to 2.78 ± 0.34 in the WT mice, measured as the mean of the three striatal regions; Fig. 4C). Specifically, the decrease in proximal spine density remains constant across the striatal gradients in Ak mice. In relation to distal spine density, we did not find differences in both SPNs of WT mice along the dorso-ventral axis (dSPN: 7.72 ± 0.58, WT dorsal; 8.13 ± 0.67, WT middle and 8.44 ± 0.79, WT ventral; iSPN: 7.25 ± 0.45, WT dorsal; 7.52 ± 1.17, WT middle and 8.44 ± 1.11, WT ventral). In addition, we also observed a gradient of distal spine density as a function of DA concentration (Fig. 4D). We first reconfirmed spine loss in the dorsal striatum of Ak mice, the area with the lowest extracellular DA levels (3.71 ± 0.33 for d-SPNs; 3.69 ± 0.28 for i-SPNs). In the partially innervated areas (middle striatum), where TH innervation is greater than in the dorsal part, spine density is intermediate (5.5 ± 0.45 in d-SPNs; 5.66 ± 0.52 in i-SPNs). The spine density in this middle striatal area of Ak mice is statistically different from the dorsal and ventral parts of the striatum. In the ventral striatum of Ak mice, as expected, there were no changes in spine density (6.73 ± 0.46 in d-SPNs; 6.64 ± 0.55 in i-SPNs) compared to WT animals (8.06 ± 0.37 in d-SPNs; 7.68 ± 0.5 in i-SPNs), since TH fibers and extracellular DA levels are similar to those in WT mice.

4.3. Striatal excitability is altered in d-SPNs

First, we did not find differences in the firing rate of both SPNs along the dorso- ventral axis in WT mice (Fig. 5A). To determine if these morphological changes correlate with striatal excitability, we studied the firing rate in Ak mice. In the middle and ventral striatum, the excitability of d-SPNs remained unchanged (Fig. 5B) while the firing rate of d-SPNs was increased in the dorsal striatum. However, there were no changes in the excitability of i-SPNs along the dorso-ventral axis (Fig. 5B). This finding indicates that significant (> 80%) loss of striatal DA terminals like that found in dorsal striatum appears necessary to induce a hyperexcitability state of d-SPNs, while i-SPNs remain less affected.

5. Discussion

The motor symptoms of PD are closely coupled with the gradual degeneration of SNc dopaminergic neurons, which induces progressive denervation of SPNs. This leads to hypoactivity of d-SPNs and hyperactivity of i-SPNs, generating a reduction in movement. The most common PD models were based on the use of neurotoxins including 6-hydroxydopamine (6-OHDA; Day et al., 2006; Zhang et al., 2013; Fieblinger et al., 2014, 2018; Suarez et al., 2014, 2016; Gagnon et al., 2017; Ketzef et al., 2017) and 1-methyl-4-phenyl-1,2,3,6-tetrahydropyridine (MPTP; Villalba et al., 2009; Toy et al., 2014). These models induce severe, almost complete striatal denervation. In contrast, clinical observations in patients suggest that motor symptoms appear when the afferent deficit is > 50% (Kordower et al., 2013). During the preclinical stage, there is a time window in which the progressive loss of the dopaminergic neurons is asymptomatic, reflecting the capacity of the system to compensate for the gradual loss of DA. It is possible that moderate levels of DA in the striatum are able to maintain the SPNs homeostatic activity and therefore delaying the appearance of motor symptoms. For this reason, the study of the morphology and functional activity in the partially innervated striatal area is essential to understand the progression of PD symptoms. The SPNs located in the partially innervated striatum are playing a critical role in the maintenance of global striatal function while dopaminergic neurons in the SNc are

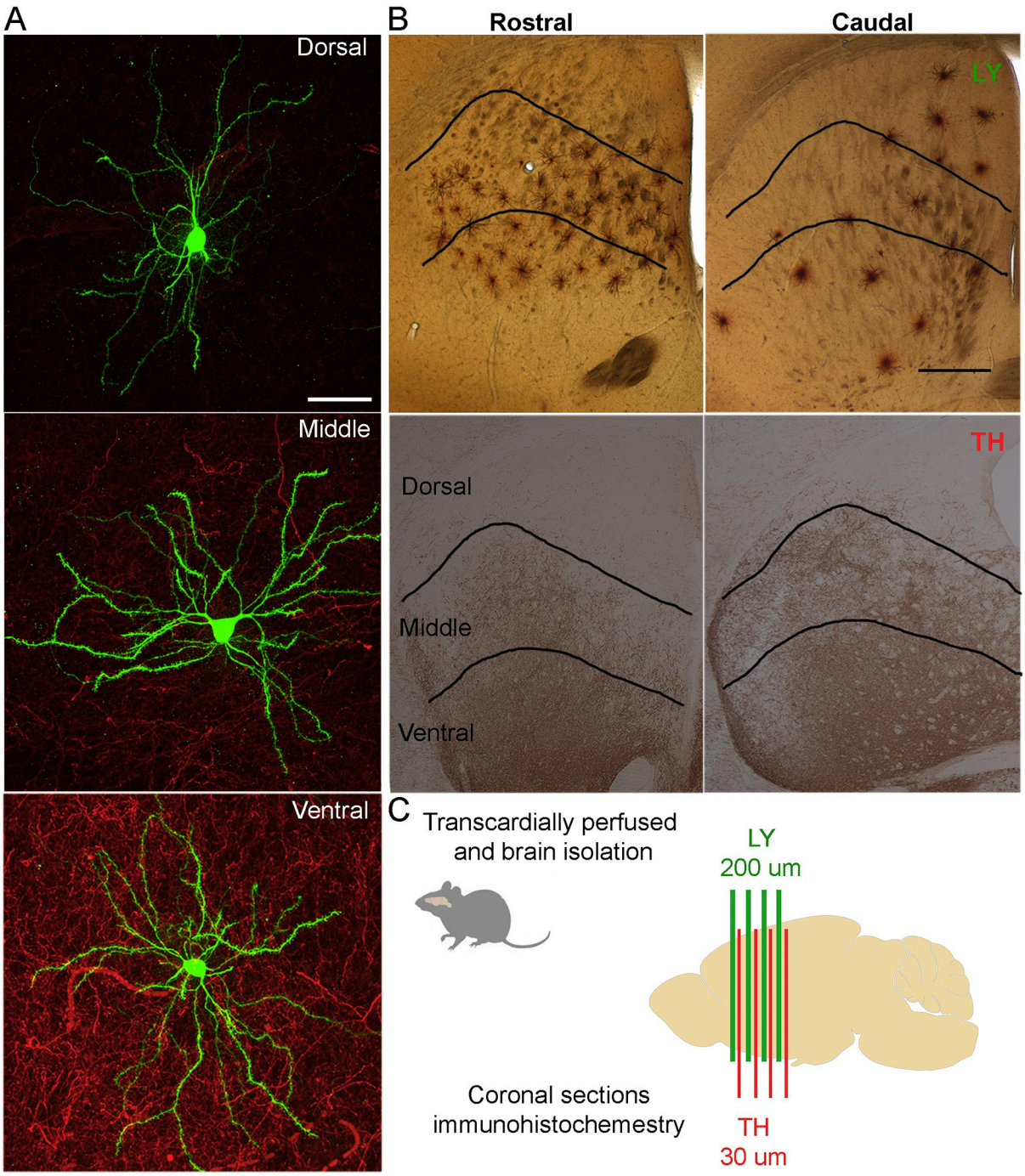

Fig. 2. 3D reconstruction of SPN and experimental design. (A) Complete morphological reconstruction of SPNs (green) in the dorsal, middle and ventral striatal areas showing low, moderate and high TH fiber innervation (red). (B) Rostro-caudal pairs of LY-intracellularly injected SPN sections with its corresponding adjacent TH-stained sections. (C) Diagram illustrating the pairing of 200 µm thick sections for LY injections with their adjacent 30 µm thick section stained with TH throughout the striatal rostro-caudal axis. Scale bar: 50 µm, A; 500 µm, B. (For interpretation of the references to color in this figure legend, the reader is referred to the web version of this article.)

degenerating.

One of the best PD mice models to study synaptic morphology in partially innervated striatal areas is the Ak mouse, which recapitulates moderate stages of the disease in PD patients. Ak mice are deficient in the transcription factor Pitx3, affecting primarily dopaminergic neurons in the SNc, where there are only a few neurons present (Kouwenhoven et al., 2017; Smidt et al., 2004), providing partial striatal innervation. Consequently, Ak mice show impaired spontaneous locomotor activity and motor coordination (Nunes et al., 2003; Solís et al., 2015; Suarez et al., 2018, García-Montes et al., 2019). Partial TH innervation in Ak mice is distributed in a dorso-ventral gradient and provides an ideal tool to study structural and functional plasticity under conditions of different degrees of dopamine innervation. The aim of this study was to elucidate how different degrees of dopaminergic inputs modify the dendritic morphology and excitability of d-SPNs and i-SPNs. We found that Ak mice, with their dorso-ventral gradient of TH innervation, also show a dorso-ventral gradient of extracellular DA levels. Ak mice have low extracellular DA levels in the dorsal striatum, where there is low TH innervation, moderate or intermediate extracellular DA levels in the middle, where TH innervation ranges from 50 to 70%, and extracellular

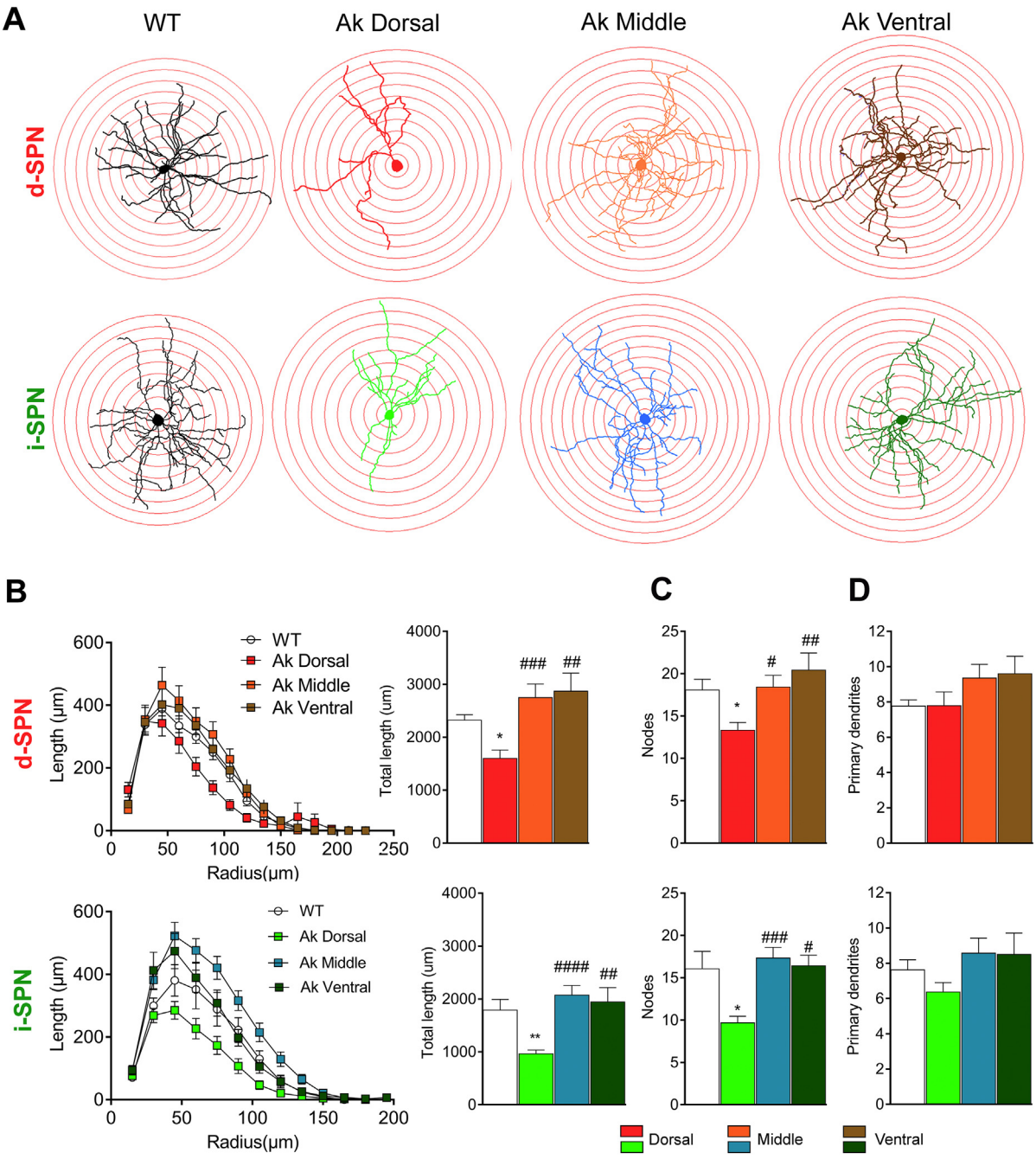

Fig. 3. Morphological changes of d-SPNs and i-SPNs along the striatal dorso-ventral gradient of TH innervation. (A) Representative drawings of the Sholl length. (B) Sholl analysis of length of d-SPNs (top left) and total length (top right) in WT (n = 23 neurons) and in Ak mice, dorsal (n = 24), middle (n = 23) and ventral (n = 9). Sholl analysis of length of i-SPNs (bottom left) and total length (bottom right) of i-SPNs in WT (n = 17 neurons) and in Ak mice, dorsal (n = 19 neurons), middle (n = 20) and ventral (n = 10 neurons). (C) Number of nodes of d-SPNs (top) and i-SPNs (bottom). (D) Number of primary dendrites of d-SPNs (top) and i-SPNs (bottom).
Significant differences were established by one-way ANOVA followed by Bonferroni's test at $^{*}p < .05$, $^{**}p < .01$ vs. WT; $^{\#}$ p < .05, $^{\#\#}$ p < .01, $^{\#\#\#}$ p < .001 vs. Ak Dorsal.

DA levels similar to WT in the ventral areas, where innervation is comparable to WT animals. According to these gradients, changes in structural plasticity in both d-SPNs and i-SPNs are directly correlated with extracellular DA levels. However, in agreement with previous results (Lieberman et al., 2018), only the d-SPNs in the dorsal striatum (with a severe lack of DA) increase their excitability.

The number of nodes and the size of the arbor tree in d-SPNs and i-SPNs are maintained through intermediate and normal levels of DA (in the middle and ventral striatum, respectively). One possibility is that dendritic atrophy occurs by an "all or none" phenomenon. These results are in agreement with the findings of Tiroshi and Goldberg (2019) that indicate that the dendritic tree has a critical role in maintaining the basal ganglia system.

The different morphology changes in both types of striatal projection neurons are still hotly debated. We show that the two striatal neurons respond similarly to DA changes probably because both receive similar dopaminergic innervation from the SN. Interestingly, we observed a drastic reduction of proximal spines (< 45 µm) in SPNs along the dorso-ventral axis, independent of the dopamine gradient. Thus, it is difficult to understand why in proximal dendrites, spine density is

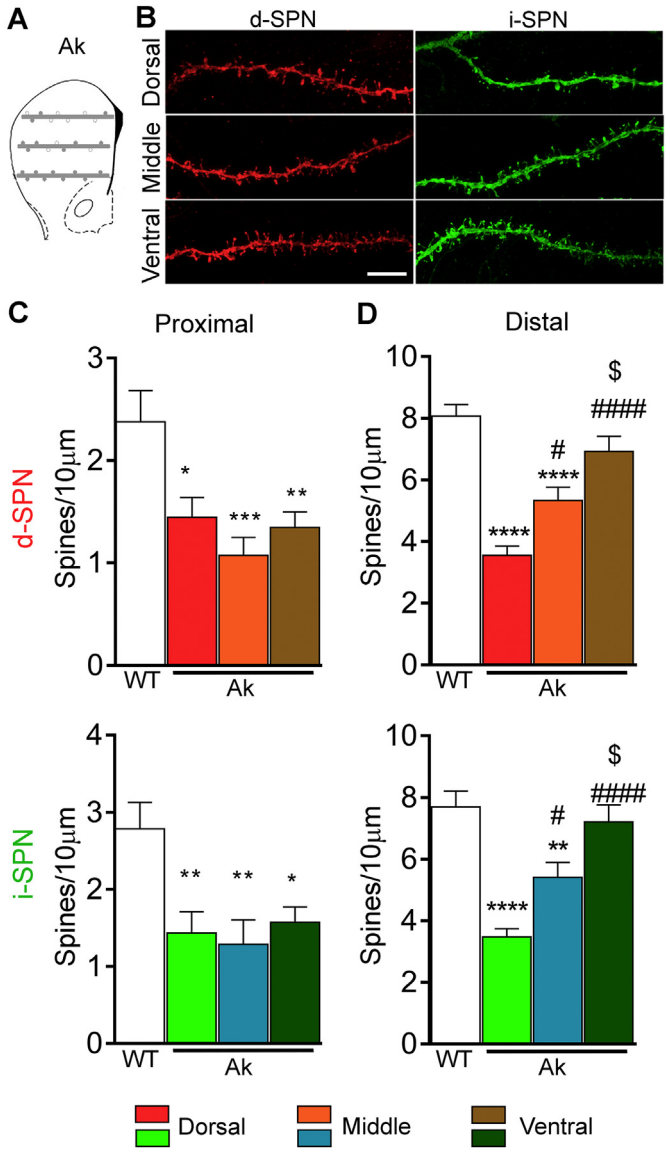

Fig. 4. Spine density gradient along the dorso-ventral striatal axis in Ak mice. (A) Representative diagram of spine density in the striatum. (B) Confocal images along the dorso-ventral striatal axis of dendrites of SPNs in Ak mice. Proximal (C) and distal (D) spine density of d-SPNs (top) in WT (n = 20) and in Ak mice, dorsal (n = 21), middle (n = 19) and ventral (n = 18) and i-SPN (bottom) in WT (n = 14) and in Ak mice, dorsal (n = 17), middle (n = 15) and ventral (n = 14).
Significant differences were established by one-way ANOVA followed by Bonferroni's test at *p < .05, **p < .01, ***p < .001 vs. WT; $^{\#}$ p < .05, $^{\#\#}$ p < .01, $^{\#\#\#\#}$ p < .01 vs. Ak dorsal; $^{\$}$p < .05 vs Ak middle.

similarly reduced in dorsal, middle and ventral striatum. One possibility is that there may be sparse dopaminergic innervation in the proximal dendrites (< 45 µm) and spine density in this region could be modulated by other factors. Findings from Villalba et al. (2013) show a significant decrease in the total number of glutamatergic terminals in the putamen of MPTP-treated parkinsonian monkeys. SPNs undergo complex pathologic modifications of glutamatergic synapses in response to dopaminergic denervation. Another possibility is the interaction between the astrocytes and SPNs. On the one hand, Martín et al. (2015) demonstrate the existence of functional astro-neuronal networks that comprise two distinct subpopulations of astrocytes in the striatum that communicate selectively with distinct populations of SPNs. However, the role of this bi-directional communication between astrocytes and neurons in PD is unknown. Moreover, there is an increase in the extent of glial coverage of striatal glutamatergic synapses in parkinsonian monkeys and the astroglial processes are much tighter and continuous than in WT animals (Villalba and Smith, 2011).

A body of evidence supports the pivotal role of dopamine in spine growth. For instance, Ingham and colleagues first demonstrated a drastic decrease of spine density in the dopamine-depleted striatum in the 6-OHDA model (Ingham et al., 1989), an effect also observed in PD patients (Zaja-Milatovic et al., 2005). Conversely, Robinson and Kolb (1997) observed that amphetamine administration, which increases dopamine in the synapse, produced an increase in the number of spines in SPNs. Supporting these studies, restoring dopamine levels in PD with its precursor L-3,4-dihydroxyphenylalanine (L-DOPA) induces spine growth in i-SPNs (Scholz et al., 2008; Fieblinger et al., 2014; Suarez et al., 2014, 2016, 2018). Experiments with cultured SPNs have shown that DA increases the number of spines (Fasano et al., 2013) and finally, Yagishita et al. (2014) reported that spine enlargement is mediated by DA. These authors found a temporal window of DA actions on the structural plasticity of dendritic spines. Together, our results support a direct link between DA and structural plasticity in the striatum in a DA concentration-dependent manner.

The impact of dopamine loss on SPN excitability is still a matter of controversy. Several authors have shown hyperexcitability of d-SPNs in different PD animal models (Fieblinger et al., 2014, 2018; Lieberman et al., 2018; Maurice et al., 2015; Suarez et al., 2014; Suarez et al. 2018). However, the same authors have found different results regarding the spike rate of i-SPNs. Lieberman et al. (2018) and Maurice et al. (2015) did not find changes in i-SPN excitability in PD mouse models compared with WT mice. Suarez et al. (2014, 2018) showed an increase of burst firing of i-SPNs, however, Fieblinger et al. (2014) found i-SPNs had lower spike rates than those in WT mice.

Here, we found an increase in the intrinsic excitability of d-SPNs in the dorsal striatum while, in the middle and ventral striatum, the excitability of d-SPNs was unchanged. Singh et al. (2016) demonstrated increased burst firing of SPNs in PD patients, but in their study, the two populations of striatal neurons could not be distinguished. However, in PD animal models, in agreement with our results, the lack of DA in the dorsal striatum induces hyperexcitability in d-SPNs (Fieblinger et al., 2014, 2018; Suarez et al., 2018). Indeed, the lack of D1R stimulation facilitates corticostriatal synapses and an increasing firing rate. The imbalance between d-SPN and i-SPN excitability could be due to thalamostriatal transmission, because post-mortem studies in PD patients (Henderson et al., 2000) and MPTP models (Villalba et al., 2014) have shown neuronal death in the intralaminar thalamic nuclei. Another explanation could be increased serotonergic striatal innervation, because there is gradual serotonin hyperinnervation inversely related to the dorso-ventral DA gradient (Li et al., 2013).

In i-SPNs, the regulation of firing rate could be tuned by homeostatic mechanisms to maintain global striatal activity. The excitability of i-SPNs is not increased in the totally denervated area, in agreement with Lieberman et al. (2018) that used young mice (p28). We recently demonstrated that i-SPNs show an increased firing rate in the dorsal striatum of Ak mice (Suarez et al., 2018). In that study, experiments were performed in three to four-month-old mice. Here, we performed electrophysiological recordings in one to three-month-old mice. According to our results from a previous study (Suarez et al., 2018) where we used 3–4 months old Ak mice, in contrast to the 1–3 month old Ak mice used here, it is possible that prolonged reductions in striatal DA lead to SPN spine loss and subsequently an increase in the neural excitability. The age-dependent susceptibility of i-SPN excitability to PD-like dopaminergic degeneration might have implications for the understanding of the pathophysiology of PD. Findings from van den Munckhof et al. (2003) demonstrate that early differentiation of dopaminergic neurons is not highly dependent on the Pitx3 gene. However, survival of these neurons requires significant Pitx3 expression. It is possible that i-SPN are less vulnerable that d-SPN to the lack of DA

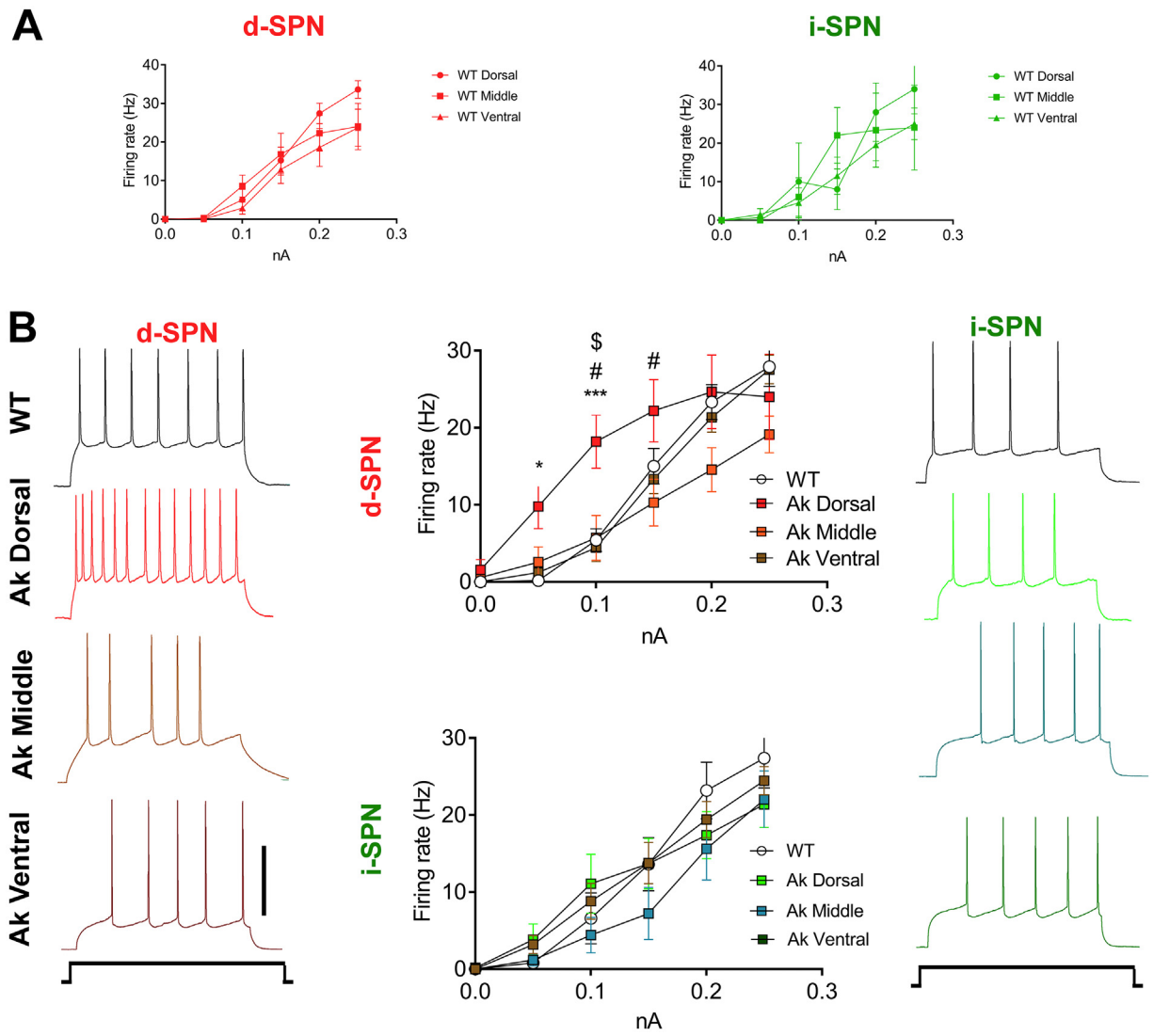

Fig. 5. Changes in the excitability of d-SPN in Ak mice. (A) Firing rate of d-SPN WT mice (WT dorsal n = 10 neurons, WT middle *n* = 7 neurons and WT ventral n = 7 neurons) and i-SPN WT mice (WT dorsal n = 3 neurons, WT middle n = 3 neurons and WT ventral *n* = 4 neurons).
(B) Representative SPN spikes evoked by depolarizing current pulse (500 ms) in d- and i-SPNs of WT (measured as the mean of the three WT striatal regions) and Ak mice in the dorsal, middle and ventral striatum (Right and left panels). Note the increase of neuronal excitability of d-SPNs in the dorsal region of Ak animals. Middle panel, Firing rate after injecting depolarizing current steps of d-SPNs (WT n = 24 neurons, Ak dorsal n = 9 neurons, Ak middle n = 7 neurons and Ak ventral *n* = 8 neurons) and i-SPNs (WT n = 10 neurons, Ak dorsal *n* = 13 neurons, Ak middle *n* = 5 neurons and Ak ventral n = 17 neurons). Two-way ANOVA followed by a Bonferroni test showed significant differences in d-SPNs for genotype ($F_{3,270} = 7.50$, $P < .01$) and for current values ($F_{5,270} = 50.44$, $P < .001$). Significant differences were established at *p < .05, **p < .01 vs. WT; # p < .05 vs. Ak dorsal, $ p < .05 vs. Ak middle. Scale bar: 50 mV.

innervation along time. Nevertheless, Van den Munckhof et al., (2003) made the experiments in postnatal 1 (P1), P21, P50 and P100 and more age-dependent experiments will be necessary to understand this phenomenon. As expected, we found that the excitability in i-SPNs in the middle and ventral striatum remained unchanged. It seems likely that a low DA concentration is sufficient to maintain the homeostatic balance in i-SPNs.

In conclusion, we have established not only that DA modulates striatal morphology, but that it does so through a DA concentration-dependent manner. This highlights the importance of regional DA concentration in the global functional striatal activity in PD patients and in animal models. These findings may have important implications for PD pathology and how SPN morphology evolves based on the stage of the illness.

Supplementary data to this article can be found online at https://doi.org/10.1016/j.nbd.2019.104666.

Acknowledgements

This work was supported by grants from the Spanish Ministries of Economía, Industria y Competitividad (SAF2016-78207-R and PCIN-2015-098) and of Sanidad Servicios Sociales e Igualdad, Instituto de Salud Carlos III (ISCIII), Centro de Investigación Biomédica en Red sobre Enfermedades Neurodegenerativas [CIBERNED] (CB06/05/0055, PNSD2016I033), the Ramón Areces Foundation (172275) to R.M. and BFU2017-88393-P from the Ministerio de Ciencia, Innovación y Universidades (MCIU), to E.D.M. We are very grateful to Dr. Oscar Solís for his critical comments on the manuscript. We would like to thank Dr. J. DeFelipe for providing the Lucifer yellow antibody.

Declaration of Competing of Interest

The authors declare no competing financial interests.

References

Albin, R.L., Young, A.B., Penney, J.B., 1989. The functional anatomy of basal ganglia disorders. Trends Neurosci. 12, 366–375.

Ares-Santos, S., Granado, N., Oliva, I., O'Shea, E., Martin, E.D., Colado, M.I., Moratalla, R., 2012. Dopamine D(1) receptor deletion strongly reduces neurotoxic effects of methamphetamine. Neurobiol. Dis. 45, 810–820.

Ares-Santos, S., Granado, N., Espadas, I., Martinez-Murillo, R., Moratalla, R., 2014. Methamphetamine causes degeneration of dopamine cell bodies and terminals of the nigrostriatal pathway evidenced by silver staining. Neuropsychopharmacology 39, 1066–1080.

Armstrong-James, M., Millar, J., 1979. Carbon fibre microelectrodes. J. Neurosci. Methods 1, 279–287.

Day, M., Wang, Z., Ding, J., An, X., Ingham, C.A., Shering, A.F., Wokosin, D., Ilijic, E., Sun, Z., Sampson, A.R., Mugnaini, E., Deutch, A.Y., Sesack, S.R., Arbuthnott, G.W., Surmeier, D.J., 2006. Selective elimination of glutamatergic synapses on striatopallidal neurons in Parkinson disease models. Nat. Neurosci. 9, 251–259.

Fasano, C., Bourque, M.J., Lapointe, G., Leo, D., Thibault, D., Haber, M., Kortleven, C., Desgroseillers, L., Murai, K.K., Trudeau, L.E., 2013. Dopamine facilitates dendritic spine formation by cultured striatal medium spiny neurons through both D1 and D2 dopamine receptors. Neuropharmacology 67, 432–443.

Fieblinger, T., Graves, S.M., Sebel, L.E., Alcacer, C., Plotkin, J.L., Gertler, T.S., Chan, C.S., Heiman, M., Greengard, P., Cenci, M.A., Surmeier, D.J., 2014. Cell type-specific plasticity of striatal projection neurons in parkinsonism and L-DOPA-induced dyskinesia. Nat. Commun. 5, 5316.

Fieblinger, T., Zanetti, L., Sebastianutto, I., Breger, L.S., Quintino, L., Lockowandt, M., Lundberg, C., Cenci, M.A., 2018. Striatonigral neurons divide into two distinct morphologicalphysiological phenotypes after chronic L-DOPA treatment in parkinsonian rats. Sci. Rep. 8, 10068.

Gagnon, D., Petryszyn, S., Sanchez, M.G., Bories, C., Beaulieu, J.M., De Koninck, Y., Parent, A., Parent, M., 2017. Striatal neurons expressing D1 and D2 receptors are morphologically distinct and differently affected by dopamine denervation in mice. Sci. Rep. 7, 41432.

García-Montes, J.R., Solís, O., Enríquez-Traba, J., Ruiz-DeDiego, I., Drucker-Colín, R., Moratalla, R., 2018. Genetic knockdown of mGluR5 in striatal D1R-containing neurons attenuates L-DOPA-induced dyskinesia in Aphakia mice. Mol. Neurobiol. 56, 4037–4050.

García-Montes, J.R., Solís, O., Enríquez-Traba, J., Ruiz-DeDiego, I., Drucker-Colín, R., Moratalla, R., 2019. Genetic knockdown of mGluR5 in striatal D1R-containing neurons attenuates L-DOPA-Induced dyskinesia in aphakia mice. Mol. Neurobiol. 56, 4037–4050.

Granado, N., Lastres-Becker, I., Ares-Santos, S., Oliva, I., Martin, E.D., Cuadrado, A., Moratalla, R., 2011. Nrf2 deficiency potentiates methamphetamine-induced dopaminergic axonal damage and gliosis in the striatum. Glia 59, 1850–1863.

Graves, S.M., Surmeier, D.J., 2019. Delayed spine pruning of direct pathway spiny projection neurons in a mouse model of parkinson's disease. Front. Cell. Neurosci. 12, 13–32.

Henderson, J.M., Carpenter, K., Cartwright, H., Halliday, G.M., 2000. Degeneration of the centre median-parafascicular complex in Parkinson's disease. Ann. Neurol. 47, 345–352.

Ingham, C.A., Hood, S.H., Arbuthnott, G.W., 1989. Spine density on neostriatal neurons changes with 6-hydroxydopamine lesions and with age. Brain Res. 503, 334–338.

Ketzef, M., Spigolon, G., Johansson, Y., Bonito-Oliva, A., Fisone, G., Silberberg, G., 2017. Dopamine depletion impairs bilateral sensory processing in the striatum in a pathway-dependent manner. Neuron 94, 855–865.

Kordower, J.H., Olanow, C.W., Dodiya, H.B., Chu, Y., Beach, T.G., Adler, C.H., Halliday, G.M., Bartus, R.T., 2013. Disease duration and the integrity of the nigrostriatal system in Parkinson's disease. Brain 136, 2419–2431.

Kouwenhoven, W.M., von Oerthel, L., Smidt, M.P., 2017. Pitx3 and En1 determine the size and molecular programming of the dopaminergic neuronal pool. PLoS One 12 (8), e0182421.

Kravitz, A.V., Freeze, B.S., Parker, P.R., Kay, K., Thwin, M.T., Deisseroth, K., Kreitzer, A.C., 2010. Regulation of parkinsonian motor behaviours by optogenetic control of basal ganglia circuitry. Nature 466, 622–626.

Li, L., Qiu, G., Ding, S., Zhou, F.M., 2013. Serotonin hyperinnervation and upregulated 5-HT2A receptor expression and motor-stimulating function in nigrostriatal dopamine-deficient Pitx3 mutant mice. Brain Res. 1491, 236–250.

Lieberman, O.J., McGuirt, A.F., Mosharov, E.V., Pigulevskiy, I., Hobson, B.D., Choi, S., Frier, M.D., Santini, E., Borgkvist, A., Sulzer, D., 2018. Dopamine triggers the maturation of striatal spiny projection neuron excitability during a critical period. Neuron 99, 540–554.

Martín, E.D., Sánchez-Perez, A., Trejo, J.L., Martin-Aldana, J.A., Cano Jaimez, M., Pons, S., Acosta Umanzor, C., Menes, L., White, M.F., Burks, D.J, 2012. IRS-2 Deficiency impairs NMDA receptor-dependent long-term potentiation. Cereb. Cortex. 22 (8), 1717–1727.

Martín, R., Bajo-Grañeras, R., Moratalla, R., Perea, G., Araque, A., 2015. Circuit specific signaling in astrocyte-neuron networks in basal ganglia pathways. Science 349, 730–734.

Maurice, N., Liberge, M., Jaouen, F., Ztaou, S., Hanini, M., Camon, J., Deisseroth, K., Amalric, M., Kerkerian-Le, G.L., Beurrier, C., 2015. Striatal cholinergic interneurons control motor behavior and basal ganglia function in experimental parkinsonism. Cell Rep. 13, 657–666.

McNeill, T.H., Brown, S.A., Rafols, J.A., Shoulson, I., 1988. Atrophy of medium spiny I striatal dendrites in advanced Parkinson's disease. Brain Res. 455, 148–152.

Nishijima, H., Suzuki, S., Kon, T., Funamizu, Y., Ueno, T., Haga, R., Suzuki, C., Arai, A., Kimura, T., Suzuki, C., Meguro, R., Miki, Y., Yamada, J., Migita, K., Ichinohe, N., Ueno, S., Baba, M., Tomiyama, M., 2014. Morphologic changes of dendritic spines of striatal neurons in the levodopa-induced dyskinesia model. Mov. Disord. 29, 336–343.

Nunes, I., Tovmasian, L.T., Silva, R.M., Burke, R.E., Goff, S.P., 2003. Pitx3 is required for development of substantia nigra dopaminergic neurons. Proc. Natl. Acad. Sci. U. S. A. 100, 4245–4250.

Oliva, I., Fernández, M., Martín, E.D., 2013. Dopamine release regulation by astrocytes during cerebral ischemia. Neurobiol. Dis. 58, 231–241.

Robinson, T.E., Kolb, B., 1997. Persistent structural modifications in nucleus accumbens and prefrontal cortex neurons produced by previous experience with amphetamine. J. Neurosci. 17, 8491–8497.

Scholz, B., Svensson, M., Alm, H., Sköld, K., Fälth, M., Kultima, K., Guigoni, C., Doudnikoff, E., Li, Q., Crossman, A.R., Bezard, E., Andrén, P.E., 2008 Feb 13. Striatal proteomic analysis suggests that first L-dopa dose equates to chronic exposure. Plos one 3 (2), e1589.

Singh, A., Mewes, K., Gross, R.E., DeLong, M.R., Obeso, J.A., Papa, S.M., 2016 Aug 23. Human striatal recordings reveal abnormal discharge of projection neurons in Parkinson's disease. Proc. Natl. Acad. Sci. U S A. 113 (34), 9629–9634.

Smidt, M.P., Smits, S.M., Bouwmeester, H., Hamers, F.P., van der Linden, A.J., Hellemons, A.J., Graw, J., Burbach, J.P., 2004. Early developmental failure of substantia nigra dopamine neurons in mice lacking the homeodomain gene Pitx3. Development 131, 1145–1155.

Solís, O., Limón, D.I., Flores-Hernández, J., Flores, G., 2007. Alterations in dendritic morphology of the prefrontal cortical and striatum neurons in the unilateral 6-OHDA-rat model of Parkinson's disease. Synapse 61, 450–458.

Solís, O., Espadas, I., Del-Bel, E.A., Moratalla, R., 2015. Nitric oxide synthase inhibition decreases l-DOPA-induced dyskinesia and the expression of striatal molecular markers in Pitx3(−/−) aphakia mice. Neurobiol. Dis. 73, 49–59.

Suarez, L.M., Solis, O., Carames, J.M., Taravini, I.R., Solis, J.M., Murer, M.G., Moratalla, R., 2014. L-DOPA treatment selectively restores spine density in dopamine receptor D2- expressing projection neurons in dyskinetic mice. Biol. Psychiatry 75, 711–722.

Suarez, L.M., Solis, O., Aguado, C., Lujan, R., Moratalla, R., 2016. L-DOPA oppositely regulates synaptic strength and spine morphology in D1 and D2 striatal projection neurons in dyskinesia. Cereb. Cortex 26, 4253–4264.

Suarez, L.M., Alberquilla, S., Garcia-Montes, J.R., Moratalla, R., 2018. Differential synaptic remodeling by dopamine in direct and indirect striatal projection neurons in Pitx3(−/−) mice, a genetic model of Parkinson's disease. J. Neurosci. 38, 3619–3630.

Tiroshi, L., Goldberg, J.A., 2019. Population dynamics and entrainment of basal ganglia pacemakers are shaped by their dendritic arbors. PLoS Comput. Biol. 15 (2), e1006782.

Toy, W.A., Petzinger, G.M., Leyshon, B.J., Akopian, G.K., Walsh, J.P., Hoffman, M.V., Vuckovic, M.G., Jakowec, M.W., 2014. Treadmill exercise reverses dendritic spine loss in direct and indirect striatal medium spiny neurons in the 1-methyl-4-phenyl-1,2,3,6- tetrahydropyridine (MPTP) mouse model of Parkinson's disease. Neurobiol. Dis. 63, 201–209.

van den Munckhof, P., Luk, K.C., Ste-Marie, L., Montgomery, J., Blanchet, P.J., Sadikot, A.F., Drouin, J., 2003. Pitx3 is required for motor activity and for survival of a subset of midbrain dopaminergic neurons. Development 130, 2535–2542.

Villalba, R.M., Smith, Y., 2011. Neuroglial plasticity at striatal glutamatergic synapses in Parkinson's disease. Front. Syst. Neurosci. 5, 68.

Villalba, R.M., Lee, H., Smith, Y., 2009. Dopaminergic denervation and spine loss in the striatum of MPTP-treated monkeys. Exp. Neurol. 215, 220–227.

Villalba, R.M., Wichmann, T., Smith, Y., 2013. Preferential loss of thalamostriatal over corticostriatal glutamatergic synapses in MPTP-treated parkinsonian monkeys. Soc. Neurosci. Annu. Meet. Abstr. 240, 02.

Villalba, R.M., Wichmann, T., Smith, Y., 2014. Neuronal loss in the caudal intralaminar thalamic nuclei in a primate model of Parkinson's disease. Brain Struct. Funct. 219, 381–394.

Yagishita, S., Hayashi- Takagi, A., Ellis- Davies, G.C., Urakubo, H., Ishii, S., Kasai, H., 2014. A critical time window for dopamine actions on the structural plasticity of dendritic spines. Science 345, 1616–1620.

Zaja-Milatovic, S., Milatovic, D., Schantz, A.M., Zhang, J., Montine, K.S., Samii, A., Deutch, A.Y., Montine, T.J., 2005. Dendritic degeneration in neostriatal medium spiny neurons in Parkinson disease. Neurology 64, 545–547.

Zhang, Y., Meredith, G.E., Mendoza-Elias, N., Rademacher, D.J., Tseng, K.Y., Steece-Collier, K., 2013. Aberrant restoration of spines and their synapses in L-DOPA-induced dyskinesia: involvement of corticostriatal but not thalamostriatal synapses. J. Neurosci. 33, 11655–11667.